Liquid Crystals
Publication details, including instructions for authors and subscription information:
http://www.informaworld.com/smpp/title~content=t713926090

Saddle-splay and mechanical instability in nematics confined to a cylindrical annular geometry

P. Palffy-muhoray[a]; A. Sparavigna[b]; A. Strigazzi[b]
[a] Liquid Crystal Institute and Department of Physics, Kent State University, Kent, Ohio, U.S.A. [b] Dipartimento di Fisica, Politecnico di Torino, G.N.S.M.-C.I.S.M. and I.N.F.M., Unità di Torino, Torino, Italy

To cite this Article Palffy-muhoray, P. , Sparavigna, A. and Strigazzi, A.(1993) 'Saddle-splay and mechanical instability in nematics confined to a cylindrical annular geometry', Liquid Crystals, 14: 4, 1143 — 1151
To link to this Article: DOI: 10.1080/02678299308027822
URL: http://dx.doi.org/10.1080/02678299308027822

LIQUID CRYSTALS, 1993, VOL. 14, NO. 4, 1143–1151

Saddle-splay and mechanical instability in nematics confined to a cylindrical annular geometry

by P. PALFFY-MUHORAY†, A. SPARAVIGNA‡
and A. STRIGAZZI*‡

† Liquid Crystal Institute and Department of Physics,
Kent State University, Kent, Ohio 44242, U.S.A.
‡ Dipartimento di Fisica, Politecnico di Torino,
G.N.S.M.-C.I.S.M. and I.N.F.M., Unità di Torino,
C.so Duca Degli Abruzzi 24, I-10129 Torino, Italy

The occurrence of a mechanical instability is predicted for a nematic liquid crystal confined to a cylindrical annular geometry. The surfaces impose either a bend distortion (azimuthal configuration) or a splay distortion (radial configuration) in the plane of the cylinders' cross-section. Remarkably, the instability appears also with strong anchoring, and, when the torsional anchoring is weak, then the saddle-splay elastic constant K_{24} deeply influences the critical radii.

1. Introduction

We consider the behaviour of a nematic liquid crystal confined to the region between two concentric cylinders such that the alignment of the director at both surfaces is either azimuthal (see figure 1) or radial (see figure 2). The mechanical stability of the corresponding configurations, where the director is locally either along the azimuthal or radial directions, is examined using linear stability theory. We find that, as the outer radius is increased, both the azimuthal and radial configurations lose their stability, and a distorted configuration becomes energetically favourable. The distortions may be out-of-plane, where the director escapes into the third dimension [1–3], or they may be in-plane. The effect of weak anchoring is to reduce the threshold for the transitions. For a certain range of parameters, bistable behaviour is found.

2. Theory

The free energy due to elastic distortions in the bulk is

$$\mathscr{F} = \int \{\tfrac{1}{2}[K_{11}(\nabla\cdot\mathbf{n})^2 + K_{22}(\mathbf{n}\cdot\nabla\times\mathbf{n})^2 + K_{33}(\mathbf{n}\times\nabla\times\mathbf{n})^2] - (K_{22}+K_{24})\nabla\cdot(\mathbf{n}(\nabla\cdot\mathbf{n}) + \mathbf{n}\times\nabla\times\mathbf{n})\}\, dV, \quad (1)$$

where K_{11}, K_{22}, K_{33} are the elastic constants of splay, twist, and bend, respectively and K_{24} is the surface-like saddle-splay elastic constant [4–6]. As shown in figures 1 and 2,

* Author for correspondence.

0267–8292/93 $10·00

the components of the director **n**, in cylindrical coordinates, are

$$\left.\begin{aligned} n_r &= \cos\theta \sin\gamma, \\ n_\phi &= \cos\theta\cos\gamma, \\ n_z &= \sin\theta, \end{aligned}\right\} \tag{2}$$

and we assume that θ and γ depend only on r, due to the symmetry.

It is useful to make the conformal transformation $r\to e^x$, $\phi\to y$ and $z\to z$. Omitting the last term in equation (1), which can be converted into a surface integral, the bulk free energy per unit length becomes

$$\frac{\mathscr{F}_{\text{bulk}}}{\pi L} = \int_{x_0}^{x_1}\left\{K_{11}\left(n_x+\frac{\partial n_x}{\partial x}\right)^2 + K_{22}\left(n_y n_x - n_y\frac{\partial n_z}{\partial x}+n_z\frac{\partial n_y}{\partial x}\right)^2 + K_{33}\left[\left(n_y^2-n_x\frac{\partial n_x}{\partial x}\right)^2+\left(n_x n_y+n_x\frac{\partial n_y}{\partial x}\right)^2+\left(n_x\frac{\partial n_z}{\partial x}\right)^2\right]\right\}dx, \tag{3}$$

where $x_0=\ln r_0$ and $x_1=\ln r_1$, and r_0 and r_1 are the radii of the inside and outside cylinders and L is the cylinder length. Since terms exist in equation (3) which are not derivatives with respect to x, the free energy may be minimized by configurations where the director field varies with x, i.e. by distortions of the radial or azimuthal configurations.

Writing the saddle splay term in equation (1) as a surface integral gives rise to the contribution to the free energy

$$\frac{\mathscr{F}_{\text{saddle-splay}}}{\pi L} = 2(K_{22}+K_{24})n_z^2|_{x_1} - 2(K_{22}+K_{24})n_z^2|_{x_0}, \tag{4}$$

we expect the free energy contributions from surface anchoring to take the form

$$\mathscr{F}_{\text{anchoring}} = \{\tfrac{1}{2}W(\mathbf{n}\cdot\mathbf{k})^2+\tfrac{1}{2}U(\mathbf{n}\cdot\mathbf{r})^2\}2\pi rL, \tag{5}$$

for each surface, where **k** and **r** are unit vectors in the axial and radial directions, and W and U are anchoring strengths. This gives

$$\frac{\mathscr{F}_{\text{anchoring}}}{\pi L} = W_0 r_0 n_z^2|_{x_0} + U_0 r_0 n_r^2|_{x_0} + W_1 r_1 n_z^2|_{x_1} + U_1 r_1 n_r^2|_{x_1}. \tag{6}$$

The bulk free energy, expanded up to quadratic terms in the angles, is

$$\frac{\mathscr{F}_{\text{bulk}}}{\pi L} = \int f_{\text{bulk}}\,dx = \int\{K_{11}(\gamma^2+\gamma'^2+2\gamma\gamma') + K_{22}(\theta^2+\theta'^2-2\theta\theta') + K_{33}(-\gamma^2-2\theta^2-2\gamma\gamma')\}\,dx, \tag{7}$$

where primes denote differentiation with respect to x, while the surface free energy is

$$\frac{\mathscr{F}_{\text{surface}}}{\pi L} = f_{\text{surface}} = [W_0 r_0 + 2(K_{22}+K_{24})]\theta^2|_{x_0} + [W_1 r_1 + 2(K_{22}+K_{24})]\theta^2|_{x_1} + U_0 r_0 \gamma^2|_{x_0} + U_1 r_1 \gamma^2|_{x_1}. \tag{8}$$

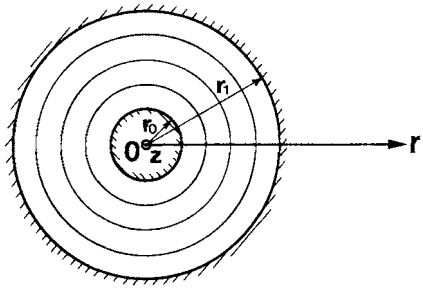

(*a*)

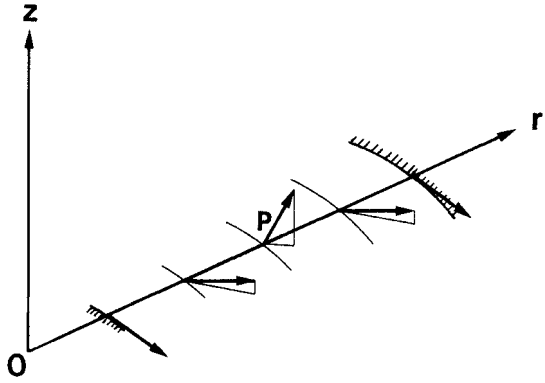

(*b*)

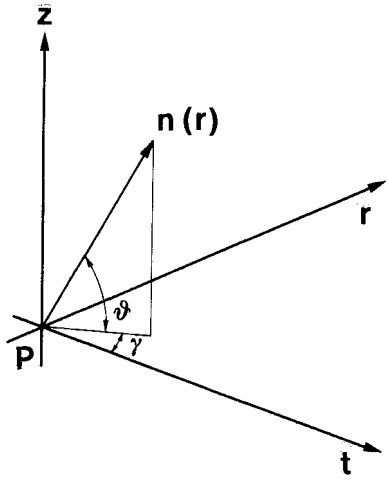

(*c*)

Figure 1. Azimuthal configuration (*a*) director profile in the undisturbed initial bend distortion; (*b*) above the thresholds for both axial escape and in-plane splay deformation; (*c*) local director $\mathbf{n}(P)$ at the arbitrary point $P(r)$ with the twist angle $\theta(r)$ and the tilt angle $\gamma(r)$ in the local frame.

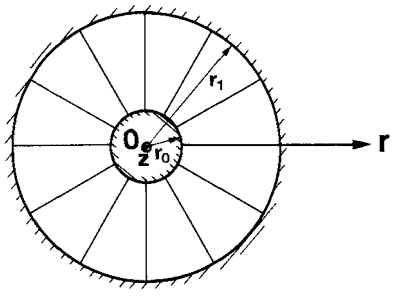

(*a*)

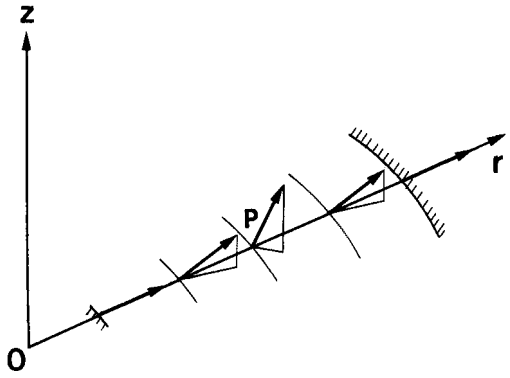

(*b*)

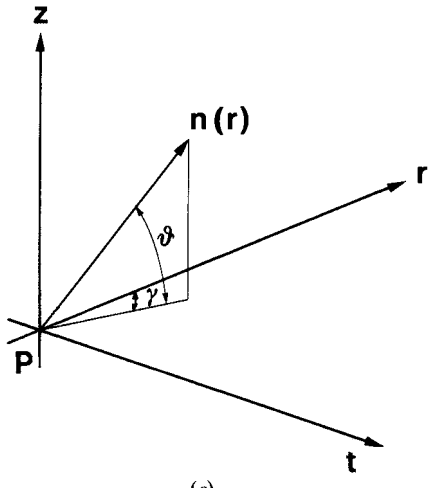

(*c*)

Figure 2. Radial configuration (*a*) director profile in the undisturbed initial splay distortion; (*b*) above the thresholds for both axial escape and in-plane bend deformation; (*c*) local director $\mathbf{n}(P)$ at the arbitrary point $P(r)$ with the bend angle out-of-plane $\theta(r)$ and the bend angle in-plane $\gamma(r)$, in the local frame.

Linear stability analysis is carried out as follows. The dynamical Landau–Khalatnikov equations describing the evolution of a given configuration are

$$\left.\begin{aligned} \mu\frac{\partial\theta}{\partial t} &= -\frac{\delta f_{\text{tot}}}{\delta\theta}, \\ \text{and} \qquad \nu\frac{\partial\gamma}{\partial t} &= -\frac{\delta f_{\text{tot}}}{\delta\gamma}, \end{aligned}\right\} \tag{9}$$

where μ and ν are viscosities, and $(\delta f_{\text{tot}}/\delta\theta)$ and $(\delta f_{\text{tot}}/\delta\gamma)$ are the first variations of the total free energy density with respect to θ and γ. Assuming that $\gamma(t,x)=\exp(\lambda t)\gamma(x)$, this gives

$$\gamma''+\Omega^2\gamma=0, \tag{10}$$

where

$$\Omega^2=\left(\frac{K_{33}}{K_{11}}-1\right)-\nu\lambda.$$

The boundary conditions are

$$\left.\begin{aligned} \frac{\partial f_{\text{bulk}}}{\partial\gamma'}+\frac{\partial f_{\text{surface}}}{\partial\gamma} &= 0|_{x_1}, \\ \text{and} \qquad -\frac{\partial f_{\text{bulk}}}{\partial\gamma'}+\frac{\partial f_{\text{surface}}}{\partial\gamma} &= 0|_{x_0}, \end{aligned}\right\} \tag{11}$$

and similarly for θ. In the case of strong anchoring, this gives $\Omega(x_1-x_0)=m\pi$, where m is an integer $\neq 0$. Then

$$\nu\lambda=\left(\frac{K_{33}}{K_{11}}-1\right)-\frac{m^2\pi^2}{(x_1-x_0)^2}, \tag{12}$$

and the system is unstable if $\lambda>0$.

In the case of strong anchoring, the thresholds for the mechanical instabilities are as follows:

$$r_1=r_0\exp\left(\frac{\pi}{\omega_c}\right), \tag{13}$$

where ω_c is given by

$$\left.\begin{aligned} \omega_c &= \left(\frac{2K_{33}}{K_{22}}-1\right)^{1/2} \qquad \text{escape (twist) distortion,} \\ \text{and} \qquad \omega_c &= \left(\frac{K_{33}}{K_{11}}-1\right)^{1/2} \qquad \text{splay (in-plane) distortion,} \end{aligned}\right\} \tag{14}$$

for the azimuthal configuration, whereas for the radial configuration the corresponding thresholds:

$$\left.\begin{aligned} \omega_c &= \left(\frac{K_{11}}{K_{33}}\right)^{1/2} \qquad \text{escape (axial bend) distortion,} \\ \text{and} \qquad \omega_c &= \left(\frac{K_{11}}{K_{33}}-1\right)^{1/2} \qquad \text{bend (in-plane) distortion,} \end{aligned}\right\} \tag{15}$$

are obtained.

In the case of weak anchoring, the threshold is given by

$$r_1 = r_0 \exp\left\{\frac{\pi}{\omega_c}\left[1+\frac{1}{\pi}\left(\tan^{-1}\frac{\omega_c}{\epsilon_0}-\tan^{-1}\frac{\omega_c}{\epsilon_1}\right)\right]\right\}, \tag{16}$$

where, for the azimuthal configuration, ω_c, ϵ_0 and ϵ_1 are given by the following equations:

$$\left.\begin{aligned}
&\omega_c = \left(\frac{2K_{33}}{K_{22}}-1\right)^{1/2} \qquad \text{escape (twist) distortion,}\\
&\epsilon_0 = -1+2\left(1+\frac{K_{24}}{K_{22}}\right)-\frac{W_0 r_0}{K_{22}},\\
&\text{and}\\
&\epsilon_1 = -1+2\left(1+\frac{K_{24}}{K_{22}}\right)+\frac{W_1 r_1}{K_{22}},\\
&\omega_c = \left(\frac{K_{33}}{K_{11}}-1\right)^{1/2} \qquad \text{splay (in-plane) distortion,}\\
&\epsilon_0 = 1-\frac{K_{33}}{K_{11}}-\frac{U_0 r_0}{K_{11}},\\
&\text{and}\\
&\epsilon_1 = 1-\frac{K_{33}}{K_{11}}+\frac{U_1 r_1}{K_{11}},
\end{aligned}\right\} \tag{17}$$

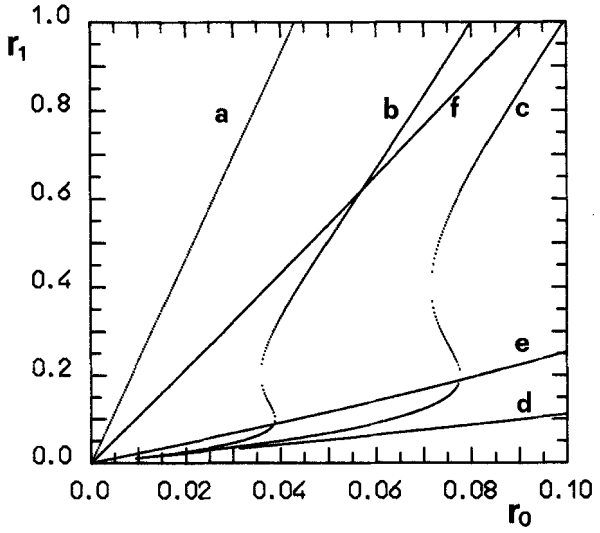

Figure 3. Critical outer radius r_1 versus the internal radius r_0 (in arbitrary units) for the tilt in-plane instability. We assume the bulk bend-splay elastic ratio $K_{33}/K_{11}=2$. The different curves are characterized by the inverse extrapolation lengths ($u_0 = U_0/K_{11}$, $u_1 = U_1/K_{11}$) at the inner and outer surfaces, respectively: a(∞, ∞); b(10, 10); c(5, 5); d(1, 1); e(∞, 1); f(1, ∞). Note that by diminishing the anchoring strength, the instability threshold decreases (a→b→c→d), and a bistability occurs for intermediate anchoring energies. It is interesting to note that the threshold is lower for case e, where anchoring is weak only at the inner surface, than in case f, where it is weak at the outer surface.

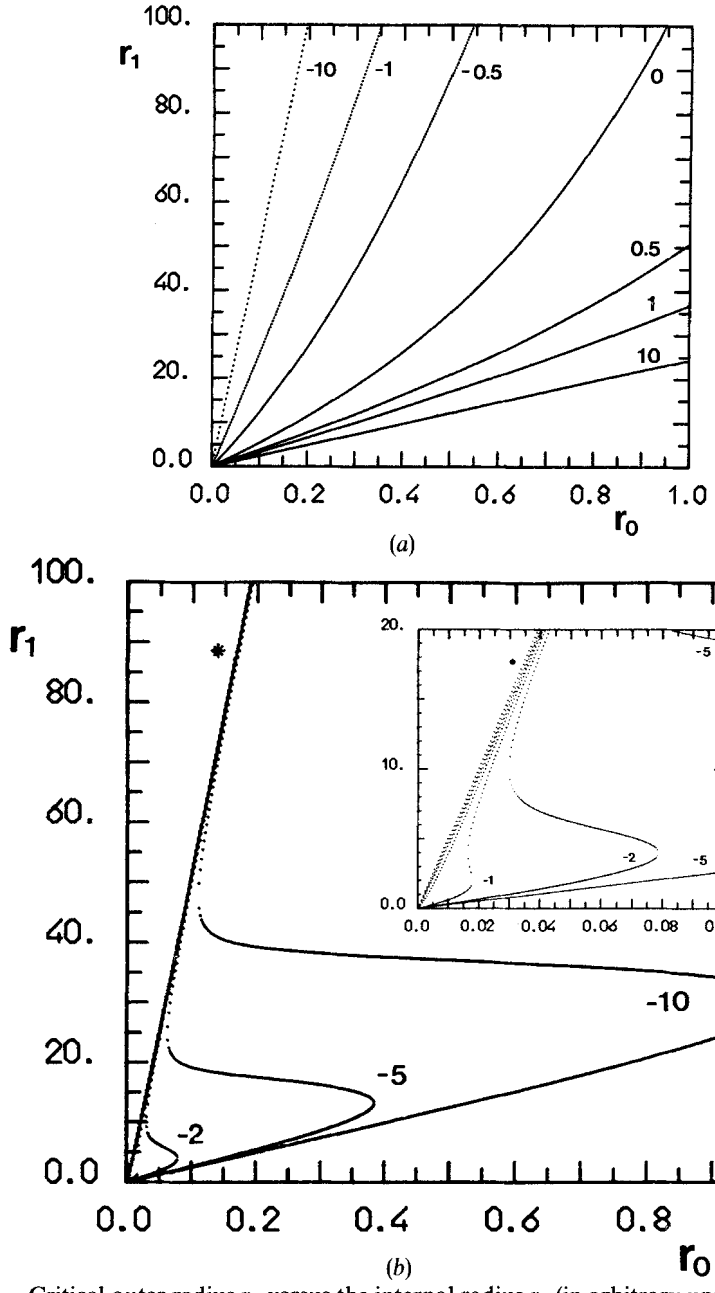

Figure 4. Critical outer radius r_1 versus the internal radius r_0 (in arbitrary units), for the axial escape instability, where the director twists out-of-plane. We assume the bulk bend-splay elastic ratio $K_{33}/K_{11}=1$. The different curves are characterized by the surface-like elastic ratio K_{24}/K_{22}, in the range $(-10, 10)$. (*a*) The outer anchoring is strong, whereas the internal one is weak ($w_0=W_0/K_{22}=1$, inverse r units). The threshold for axial escape increases with K_{24}/K_{22}. The strong anchoring at the external wall prevents bistability. (*b*) The inner anchoring is strong, whereas the outer one is weak ($w_1=W_1/K_{22}=0{\cdot}5$, inverse r units). Here the weak anchoring at the external surface allows the occurrence of bistability. Moreover, reducing K_{24}/K_{22} lowers the threshold for the axial escape. The curve marked by * shows the behaviour of the threshold for $K_{24}/K_{22}\geqslant -1$, which is better shown in the expanded inset (*: $K_{24}/K_{22}=0$, 1, 3, 5 from right to left).

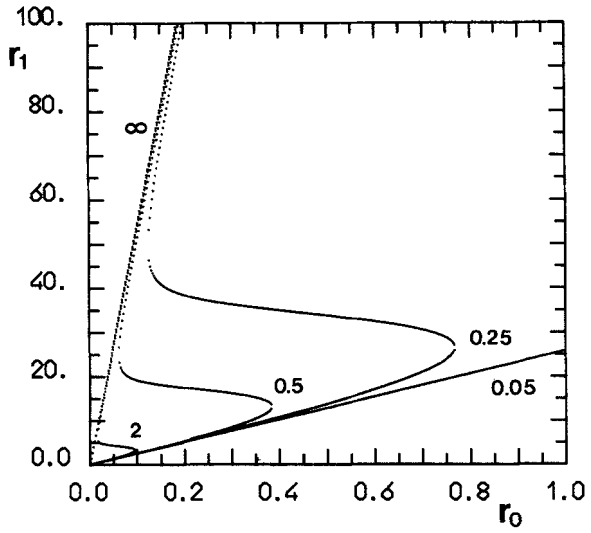

Figure 5. Critical outer radius r_1 versus the internal radius r_0 (in arbitrary units) for the axial escape instability. The bulk bend–splay elastic ratio has the same value as in figure 4, i.e. $K_{33}/K_{11}=1$. We assume the surface-like elastic ratio $K_{24}/K_{22}=-5$. The anchoring at the inner surface is strong, whereas at the outer one it has been reduced from ∞ to 0·05. Note the presence of bistability, which becomes more pronounced as the anchoring strength at the outer surface is reduced.

whereas for the radial configuration

$$\left.\begin{aligned}
&\omega_c=\left(\frac{K_{11}}{K_{33}}\right)^{1/2} \qquad \text{escape (axial bend) distortion,}\\
&\epsilon_0=-\frac{K_{11}}{K_{33}}+2\left(\frac{K_{22}}{K_{33}}+\frac{K_{24}}{K_{33}}\right)-\frac{W_0 r_0}{K_{33}}+\frac{U_0 r_0}{K_{33}},\\
&\text{and}\\
&\epsilon_1=-\frac{K_{11}}{K_{33}}+2\left(\frac{K_{22}}{K_{33}}+\frac{K_{24}}{K_{33}}\right)+\frac{W_1 r_1}{K_{33}}-\frac{U_1 r_1}{K_{33}},\\
&\omega_c=\left(\frac{K_{11}}{K_{33}}-1\right)^{1/2} \qquad \text{bend (in-plane) distortion,}\\
&\epsilon_0=1-\frac{K_{11}}{K_{33}}-\frac{U_0 r_0}{K_{33}},\\
&\text{and}\\
&\epsilon_1=1-\frac{K_{11}}{K_{33}}+\frac{U_1 r_1}{K_{33}}.
\end{aligned}\right\} \tag{18}$$

Typical threshold behaviours for the azimuthal configuration are shown in figures 3, 4 and 5.

The behaviour for the radial configuration is quite similar. In both cases, the surface-like elastic constant K_{24} plays a fundamental role in determining the threshold for the escape instability.

3. Conclusions

We have shown that the azimuthal and radial configurations of a nematic liquid crystal confined between two concentric cylinders become unstable against either escape or in-plane deformations at certain values of parameters. For the simple case of strong anchoring and in the one constant approximation, the instability occurs at the critical ratio of cylinder radii $r_1/r_0 = \exp(\pi)$ for both the azimuthal and radial [7] configurations. Both weak anchoring and the K_{24}-effect reduce the thresholds, and can lead to bistability. Some aspects of such a behaviour arise from the fact that the bulk free energy is $\propto \ln(r_1/r_0)$, while the surface terms are $\propto r_0$ and r_1. Hence for large cylinders, surface terms can dominate. These results may be useful in interpreting the behaviour of nematics in the vicinity of line defects or polymer fibres, and also in the interiors of cylindrical confining cavities, where an isotropic core could play the role of the internal cylinder.

This work was partially supported by the Ministry of the University and of the Scientific and Technical Research of the Italian Government. One of us (P.P.-M.) acknowledges support from NSF under grant DMP 89-20147 (ALCOM).

References

[1] CLADIS, P. E., and KLÉMAN, M., 1972, *J. Phys., France*, **33**, 591.
[2] MEYER, R. B., 1973, *Phil. Mag.*, **27**, 405.
[3] STRIGAZZI, A., 1989, *Nuovo Cim.* D, **10**, 1335.
[4] NEHRING, J., and SAUPE, A., 1971, *J. chem. Phys.*, **54**, 337.
[5] NEHRING, J., and SAUPE, A., 1972, *J. chem. Phys.*, **56**, 5527.
[6] BARBERO, G., SPARAVIGNA, A., and STRIGAZZI, A., 1990, *Nuovo Cim.* D, **12**, 1259, and references therein.
[7] BETHUEL, F., BREZIS, H., COLEMAN, B. D., and HELEIN, F., 1992, I.M.A. Preprint Series No. 926.